THE INFLUENCE OF A CHARGE ON A CHARGED PARTICLE FLUX

By J. TELFORD*

[*Manuscript received August* 19, 1963]

Summary

The variations in intensity of a charged particle flux when observed from a position adjacent to a point charge have been calculated. This was done to estimate the effect of a Coulomb field on charged particles in space. It is shown that for repulsion a region of complete shadow occurs which has a width, at a particular radius, dependent on the particle energy, the radial distance, and the magnitude of the scattering charge.

I. INTRODUCTION

In a recent investigation (Bigg 1963, Bowen 1963) a variation of magnetic storm frequency with lunar phase was reported. It was suggested that the effect could be due to a charge on the Moon. It thus seemed desirable to compute the disturbance to a uniformly directed flux of charged particles when the observation point moves in a plane circular path parallel to the flux and centred on the charge.

This question is similar to the classical treatment of α-particle scattering by Rutherford, but in his case the observation point was effectively at an infinite distance from the charge. Similarly, other approximate treatments all appear to take the trajectories as lying on the asymptotes of the hyperbolic path.

Here we treat the problem in two steps. Initially the scattering of a monoenergetic particle flux is dealt with and then the equations are reformulated to examine the practical case where there is a distribution of energies.

II. THE THEORETICAL MODEL

The calculation treats the case where the space charge is too small to influence the field of the fixed scattering charge. Figure 1 shows the geometry where the coordinate system is centred on the equivalent point charge. The equations of motion are (see any standard text):

$$m(\ddot{r}-(2\pi)^2 r\dot{\theta}^2) = \frac{eq}{4\pi\epsilon_0 r^2},$$

$$m\frac{1}{r}\frac{\mathrm{d}}{\mathrm{d}t}(2\pi r^2\dot{\theta}) = 0,$$

where m is the mass of the particle in kilograms and e is the charge on the particle in coulombs, r and θ are the radial coordinates in metres and decimal parts of the whole circle, q is the fixed point charge in coulombs, and

$$\epsilon_0 = 1/(36\pi\times10^9) \approx 8{\cdot}854\times10^{-12} \text{ coulombs V}^{-1}\text{ m}^{-1}.$$

* Division of Radiophysics, CSIRO, University Grounds, Chippendale, N.S.W.

These equations yield

$$\frac{b^2}{\gamma r}-\frac{b}{\gamma}\sin\theta+1-\cos\theta=0,$$

where b is the distance of the undisturbed ray from the axis as shown in Figure 1, and

$$\gamma=\frac{e}{mv_\infty^2}\frac{q}{4\pi\epsilon_0},$$

where v_∞ is the velocity of the particle before it is influenced by the charge.

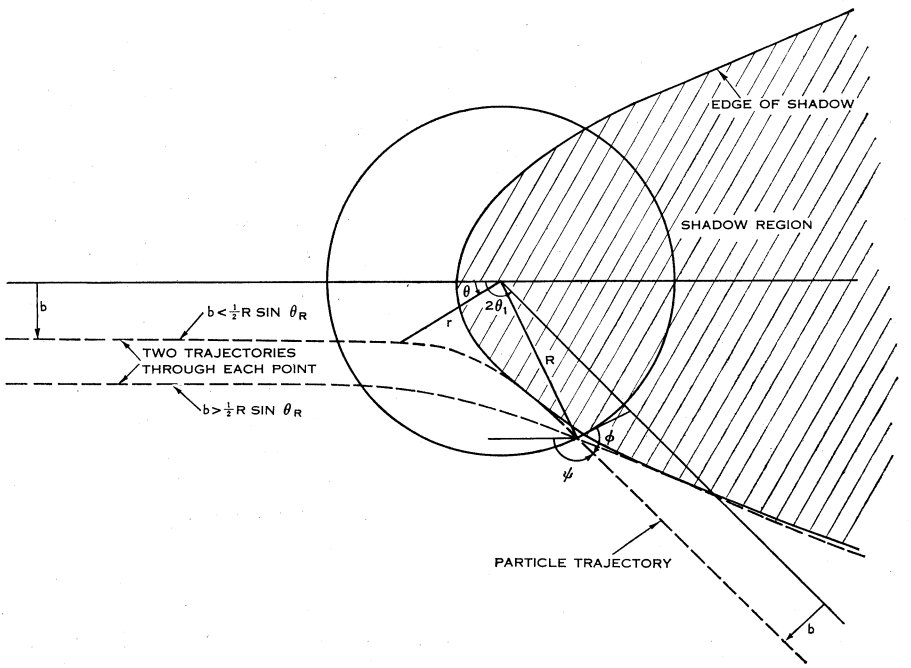

Fig. 1.—The trajectory of a typical particle is shown. It is a hyperbola with the centre of the circle as a focus. The circle includes all the points at which the flux has been calculated. The parabola shows the edge of the shadow region. The symbols are referred to in the text.

This curve is a hyperbola, asymptotic to lines parallel to $\theta=0$ and $\theta=2\theta_1$, where $\tan\theta_1=b/\gamma$. Clearly b has two possible values

$$b=\tfrac{1}{2}r\sin\theta\,[1\pm\{1-4\gamma/r(1+\cos\theta)\}^{\frac{1}{2}}],$$

and these correspond to two rays passing through each position (r,θ). If one solution b_1, is given for a particular γ, r, and θ, the other value b_2 is given by $b_2=r\sin\theta-b_1$ or $x-b_1$ in Cartesian coordinates. No real b exists if $\cos\theta+1<4\gamma/r$ and both the solutions coincide on the parabola

$$4\gamma/r=1+\cos\theta,$$

which defines a region into which none of these particles can penetrate.

The original distance from the axis of symmetry of a trajectory just touching this paraboloid at (r, θ) is $b = \frac{1}{2}r \sin\theta = \frac{1}{2}x$, in Cartesian coordinates. Thus the particle is exactly twice as far from the axis when it is at the edge of the shadow as it was when it started.

The distance of closest approach to the charge is

$$r(\text{minimum}) = \frac{\gamma(1+\cos\theta_1)}{\cos\theta_1}.$$

If the direction of the trajectory relative to the axis of symmetry is ψ ($\psi = \theta+\frac{1}{2}\pi-\phi$ radians), then we have

$$\tan\psi = \frac{1-\cos\theta}{\sin\theta - b/\gamma}.$$

The parameter γ can be interpreted physically as the value of b which gives a final deflection of 90°.

These equations describe an individual particle trajectory and may now be used to derive flux densities as a function of position in space. We assume that the incident flux density of particles when measured in terms of kinetic energy, number of particles or total charge, etc., per unit area and unit time, is everywhere constant in direction and intensity, until influenced by the fixed charge. Initially we also take particles all with the same kinetic energy. Particular energy distributions are treated later.

At any position near the charge the particles of a given energy will arrive from two directions (except on or within the parabolic shadow) and because we want to sum the two fluxes without regard to direction, the fluxes must be calculated for a surface normal to each. Continuity considerations enable us to determine the total flux coming from the area between b and $b+\delta b$ and passing out through any surface near the charge. Symmetry suggests we choose a surface S symmetric about the axis. Let the distance from the axis along S be s so that the total flux entering between b and $b+\delta b$ leaves between s and $s+\delta s$. We must now make a correction for the angle between the trajectory direction and the surface to obtain the normal flux. The obvious choice of a surface normal to the rays is laborious to formulate so here we choose the surface $r = R$. Thus $s = R\theta$ and the appropriate derivative becomes

$$\frac{\mathrm{d}b}{\mathrm{d}s} = \frac{\mathrm{d}b}{R\,\mathrm{d}\theta} = \frac{1}{R}\left(\frac{\partial b}{\partial\theta} + \frac{\partial b}{\partial r}\frac{\mathrm{d}r}{\mathrm{d}\theta}\right) = \frac{1}{R}\frac{\partial b}{\partial\theta},$$

since $\mathrm{d}r/\mathrm{d}\theta = 0$ on $r = R$.

This preference for the sphere $r = R$ should not be allowed to obscure the fact that we are dealing with a distribution function in space. However, in this context, we are interested in flux density variations as the observer moves along increasing θ on $r = R$ and so at this stage we non-dimensionalize the variables in terms of R, which is an arbitrarily selected scale radius. Thus

$$B = \frac{b}{R}, \qquad \Gamma = \frac{\gamma}{R} = \frac{e}{mv_\infty^2}\,\frac{q}{4\pi\epsilon_0 R},$$

and, on $r = R$,

$$B^2 - B\sin\theta + \Gamma(1-\cos\theta) = 0.$$

It should be noted that the problem is particularized by one parameter Γ and a change in R merely changes Γ. If $F(\theta)$ is the flux density at θ and F_0 is the undisturbed flux density

$$F(\theta) = \frac{B}{\sin\theta \sin\phi} \frac{\mathrm{d}B}{\mathrm{d}\theta} F_0,$$

where (see Fig. 1)

$$\tan\phi = \left(\frac{\mathrm{d}r}{r\mathrm{d}\theta}\right)_{r=R} = \frac{1}{B^2}(\Gamma \sin\theta - B\cos\theta)$$

and

$$\frac{\mathrm{d}B}{\mathrm{d}\theta} = \frac{\Gamma\sin\theta - B\cos\theta}{\sin\theta - 2B};$$

this is the $\mathrm{d}b/R\mathrm{d}\theta$ mentioned earlier.

One must now decide how to evaluate $F(\theta)$. Since a computer was available there was no advantage in further algebraic simplification and the problem was coded at this stage. The Sydney University computer, SILLIAC, was used and $F(\theta)$, θ, θ_1, and r(minimum), were tabulated against regular intervals in B.

III. The Case with Repulsion

A typical result is shown in Figure 2 (see also Appendix I). The two curves represent the two rays reaching each point and the curves tend to infinity at a particular value of θ beyond which none of these particles can penetrate. This is the edge of the shadow.

The maximum value of θ is given, from an earlier equation, by

$$\cos\theta_\mathrm{m} = -(1-4\Gamma).$$

The whole shadow region is a parabola of revolution in space with its apex 2γ from the charge, facing the particle flux. This is illustrated in Figure 1.

It should be noticed that the effect well away from the shadow is nearly constant with angle and is approximately $F(\theta) = (1-\Gamma)F_0$.

A further important point is that the lower curve applies to the rays which approach closest to the charge, and so if the charge is on a sphere its capture of particles has negligible effect unless the radius of the charged body is an appreciable fraction of the observational distance. This was checked by computing the minimum r for each trajectory. This is always greater than 2γ and is not significant in this context.

In the particular problem under discussion we were considering possible modifications to the proton flux from the Sun by a charge on the Moon.

In this case it is advantageous to rewrite Γ in terms of the potential, V_c, of the sphere of radius R_c which holds the charge

$$\Gamma = \frac{\gamma}{R} = \frac{e}{mv_\infty^2} \frac{R_\mathrm{c}V_\mathrm{c}}{R}.$$

For protons reaching the Earth from the Sun in 24 hours and for $\Gamma = 0{\cdot}02$ as in Figure 2 we find $V_\mathrm{c} = +60\,000$ volts is the necessary potential at the surface of the Moon.

It is interesting to note that γ may also be written

$$2\gamma = \frac{e}{\frac{1}{2}mv_\infty^2} R_c V_c = \frac{R_c V_c}{V_p},$$

where V_p is the apparent voltage used to accelerate the particles originally. Thus, when the shadow parabola just touches the sphere, $2\gamma = R_c$, $V_c = V_p$. Thence, as one expects, a sphere charged by a flux of charged particles of one sign reaches a potential equal to the accelerating potential of the particles.

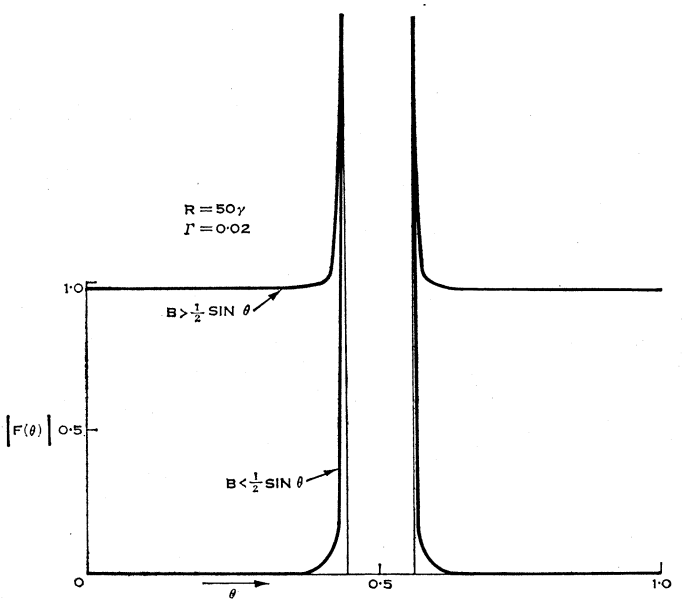

Fig. 2.—The distribution of monoenergetic particles after scattering by a point charge. The distribution shown is the flux normal to the particle rays when observed from points distance $R = 50\gamma$ (i.e. $\Gamma = 0{\cdot}02$) from the charge centre. At each observation point two rays are collected, one having suffered a large deflection from a close approach to the charge and the other proceeding more directly. The former is the lower curve in the graph. The abscissa is in angular units of the complete circle and a region of complete shadow lies behind the charge.

IV. The Theoretical Model for a Continuous Particle Energy Distribution

The infinite peaks in our previous picture are clearly associated with the delta-function energy distribution of the monoenergetic particles. A more realistic picture can only be obtained by integrating over some finite distribution. For this purpose a Gaussian distribution was selected with no particles beyond a specified energy difference from the mean. The distribution then required three parameters.

Γ_m, which defines the mean energy when the other physical parameters are included. It is *not* the mean Γ but is the Γ associated with the particle of mean energy. The subsidiary parameter γ_m is defined by $\gamma_m = R\Gamma_m$.

σ, the standard deviation of the energy distribution about the mean when the complete Gaussian curve is used, and

a, which is used to limit the calculation to energies of $(1-a\sigma)$ to $(1+a\sigma)$ times the mean value.

Thus

$$\frac{\mathrm{d}F_E}{\mathrm{d}E} = \exp[-\tfrac{1}{2}\{(E-1)/\sigma\}^2],$$

where δF_E is the flux density of particles with energies between E and $E+\delta E$ and E is the energy expressed as fractions of the average.

$$A = \left[\sqrt{2}\sigma 2^{\frac{1}{2}}\int_0^{a/\sqrt{2}} \mathrm{e}^{-t^2}\mathrm{d}t\right]^{-1}$$

is the normalizing factor necessary to make the total flux for all energies equal to unity, that is,

$$\int_{-\infty}^{+\infty} \frac{\mathrm{d}F_E}{\mathrm{d}E}\,\mathrm{d}E = A\int_{1-a\sigma}^{1+a\sigma} \exp[-\tfrac{1}{2}\{(E-1)/\sigma\}^2]\,\mathrm{d}E = 1.$$

Some difficulty arose in the integration, as no explicit expression was available for $F(\theta)$. Investigation suggested the most promising approach was to employ B as the independent variable in the integral.

Figure 3(a) shows a plot of the value of θ associated with a particular B for the Γ used to calculate Figure 2. It is seen that for a specified θ there are two values of B in most cases, but for a certain region no real B exists. These two values of B correspond to the two trajectories reaching each point, as discussed previously. If we are to integrate a range of B to cover the range of E we must be sure no attempt is inadvertently made to operate with unreal values of B.

Since we have $\bar{E} = 1/C\Gamma$,

$$C = 1/\bar{E}\Gamma_{\mathrm{m}} = 1/\Gamma_{\mathrm{m}},$$

where $\bar{E} = 1$ is the mean energy,

$$E = \frac{1-\cos\theta}{B(\sin\theta - B)}\,\Gamma_{\mathrm{m}}.$$

This is shown graphically in Figure 3(b). Thus before the integration commences the following tests are made.

1. For this θ is there a real B at $E_{\mathrm{max.}}$? If there is not, no rays reach θ and the calculation has finished if we were proceeding to calculate with θ at continually increasing values.

2. Is there a real B for $E_{\mathrm{min.}}$? If there is not, we must integrate for all values of B between the two values associated with $E_{\mathrm{max.}}$; otherwise the integration must omit the region of B associated with energies less than $E_{\mathrm{min.}}$. In practice the integration extends from B at $E_{\mathrm{max.}}$ to B at $E_{\mathrm{min.}}$ or $B = \frac{1}{2}\sin\theta$ if the latter is unreal. By starting with the smallest B and taking n equal steps to the larger end of the first subrange

of B and then substituting (sin $\theta - B$) and taking n further steps we can cover both branches automatically for every θ. It should be noted that the distribution function changes sign at $B = \frac{1}{2}\sin\theta$ because $\mathrm{d}\theta/\mathrm{d}b$ changes sign as the movement of the intersection of the ray with the circle $r = R$ for increasing b changes direction at the edge of the shadow. Since only the modulus of the distribution function is physically significant, the integral is generated after we have taken the modulus of the integrand.

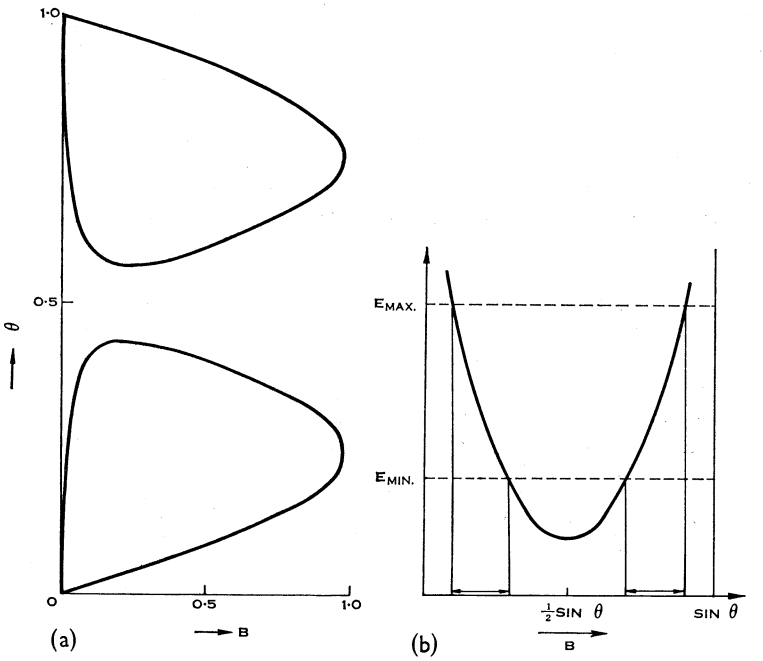

Fig. 3.—These two graphs relate the angle θ of the observation point (on the circle in this case), the initial sideways displacement of the trajectory, B, and the particle energy E. (*a*) For monoenergetic particles, where $R = 50\gamma$ (i.e. $\Gamma = 0{\cdot}02$), B and θ are related as shown. (*b*) For a given observation point θ this shows the energy necessary if the particle is to reach θ from an initial trajectory at scaled distance B from the axis. A typical integration range is marked on the abscissa.

This means we measure separately the fluxes from the two directions corresponding to the two possible ray paths and add them. This relates to a spherical charge detector which will automatically combine the two fluxes in the correct proportion, as the projected area of a sphere is insensitive to direction.

Thus the calculation generates

$$F(\theta) = \int_{E=0}^{E=+\infty} \left| X_\theta \frac{\mathrm{d}F_E}{\mathrm{d}E} \frac{\mathrm{d}E}{\mathrm{d}B} \right| \mathrm{d}B,$$

where

$$X_\theta = \frac{B}{\sin\theta \sin\phi} \frac{\mathrm{d}B}{\mathrm{d}\theta},$$

$$\tan\phi = \left(\frac{\mathrm{d}r}{r\mathrm{d}\theta}\right)_{E \text{ const.}, B \text{ const.}}$$

$$= B^{-2}\,(\Gamma\sin\theta - B\cos\theta),$$

and hence

$$\left|X_\theta \frac{\mathrm{d}E}{\mathrm{d}B}\right| = \left|\frac{E}{\sin\theta\,(\sin\theta - B)}\,[(\Gamma\sin\theta - B\cos\theta)^2 + B^4]^{\frac{1}{2}}\right|,$$

$$\mathrm{d}F_E/\mathrm{d}E = A\exp[-\tfrac{1}{2}\{(E-1)/\sigma\}^2],$$

as given earlier and is restricted to

$$\mathrm{d}F_E/\mathrm{d}E = 0, \qquad \begin{cases} E > 1-a\sigma, \\ E < 1+a\sigma. \end{cases}$$

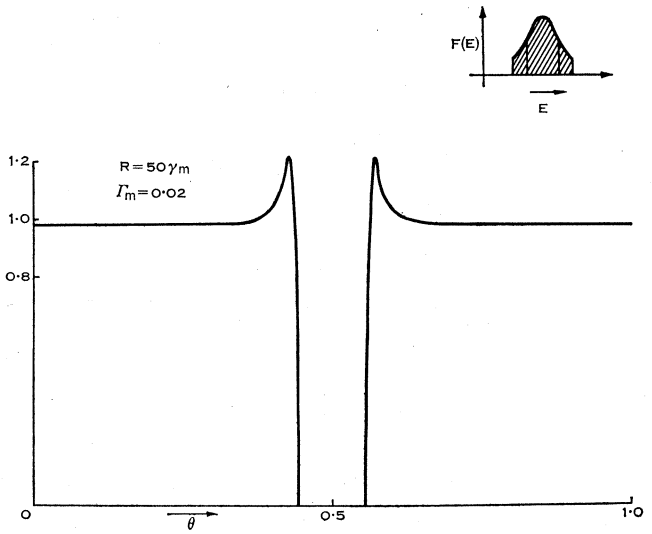

Fig. 4.—The combined flux densities from all trajectories observed at θ when the particles have the energy distribution shown in the small graph. The average energy of the particles is the same in the cases shown in Figures 4 and 5. This energy is equal to that of the monoenergetic case in Figure 2. The distribution corresponds to a radial distance of $R = 50\gamma_m$.

These calculations were also programmed on the Sydney University computer SILLIAC and three cases were calculated to illustrate the effects of a broad energy distribution.

Case (*a*).—In this case a narrow almost rectangular distribution of a width of 0·005 times the mean was used. This was to simulate the delta function and to confirm that the new program gave the same result as shown in Figure 2.

Case (*b*).—This result is shown graphically in Figure 4 and the energy distribution used is at the top right-hand corner of the figure. When we compare this with Figure 2 we see that the infinite points have been subdued but, nevertheless, a sharp peak occurs on each side of the shadow. The shadow has very steep sides with a vertical

slope at the bottom, showing that the flux is cut off very sharply. The flux away from the hole has almost the same value as in the monoenergetic case.

Case (*c*).—This is illustrated in Figure 5 and shows clearly that a very broad energy spectrum reduces the hump around the shadow and makes the onset of the shadow more gradual.

A table mapping the complete field for the energy distribution used in Figure 4 is presented in Appendix II. The program is available to anyone who requires results for other cases.

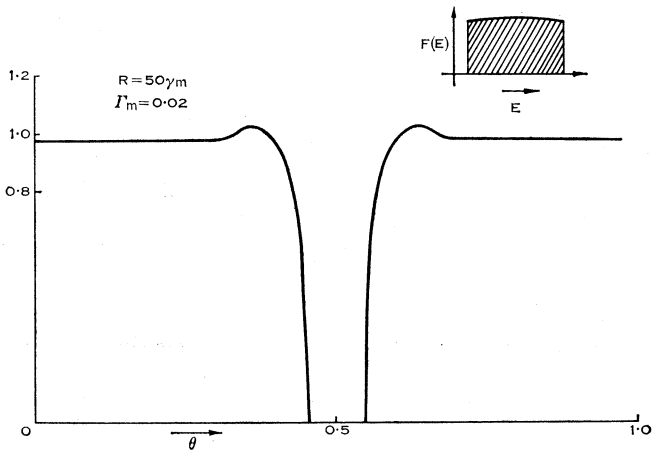

Fig. 5.—The total flux distribution when the energy distribution of the incident particles corresponds to that shown in the small graph at $R = 50\gamma_m$. This case differs from the one of Figure 4 only in the energy distribution curve.

V. Discussion

These calculations show the general features of the disturbance produced when a point charge is placed in a charged particle flux of the same sign and of negligible charge density. An accurate evaluation of the field of flux density has been made for particular energy distributions. The result is applicable to an insulated bead charged by an electron beam in a vacuum tube or to any other object carrying a Coulomb field. The shadow is complete if the particle energy has an upper limit and this corresponds to a particular shadow width. The shadow is surrounded by a narrow region of intensified flux and beyond this the flux is almost constant with a value slightly less than when undisturbed.

The calculation was done to examine the possible influence of an electrically charged Moon on solar particles. Although the distribution agrees well with observations, more direct evidence of a lunar charge is needed if the hypothesis is to be accepted as the explanation of the lunar effects discussed by Bowen and Bigg.

VI. References

Bigg, E. K. (1963).—*J. Geophys. Res.* **68**: 1409.
Bowen, E. G. (1963).—*J. Geophys. Res.* **68**: 1401.

Appendix I

I should like to thank the referee for pointing out that the algebraic solution to the monoenergetic case shown in Figure 2 is

$$\frac{F(\theta)}{F_0} = \tfrac{1}{2}(1-2/\rho)^{\frac{1}{2}}\left\{1 \pm \frac{1}{(1-4\gamma/[r(1+\cos\theta)])^{\frac{1}{2}}}\right\}.$$

Table 1

values of θ, $F(\theta)$

Q	P	0	1	2	3	4	5
	R	$2{\cdot}5\gamma_m$	$5{\cdot}0\gamma_m$	$10{\cdot}0\gamma_m$	$20{\cdot}0\gamma_m$	$40{\cdot}0\gamma_m$	$80{\cdot}0\gamma_m$
0·0	θ	0·2394	0·3273	0·3810	0·4169	0·4416	0·4588
	$F(\theta)$	0·0000	0·0000	0·0000	0·0000	0·0000	0·0000
0·1	θ	0·2276	0·3207	0·3768	0·4140	0·4396	0·4574
	$F(\theta)$	0·0936	0·1197	0·1308	0·1360	0·1385	0·1398
0·2	θ	0·1943	0·3033	0·3656	0·4064	0·4343	0·4537
	$F(\theta)$	0·3414	0·4671	0·5186	0·5425	0·5540	0·5597
0·3	θ	0·1408	0·2793	0·3508	0·3965	0·4275	0·4489
	$F(\theta)$	0·5481	0·8449	0·9584	1·0103	1·0353	1·0475
0·4	θ	0·0362	0·2521	0·3345	0·3858	0·4201	0·4438
	$F(\theta)$	0·5109	0·9519	1·1010	1·1682	1·2004	1·2161
0·5	θ		0·2221	0·3177	0·3749	0·4127	0·4387
	$F(\theta)$		0·9202	1·0788	1·1493	1·1828	1·1993
0·6	θ		0·1873	0·2999	0·3635	0·4050	0·4333
	$F(\theta)$		0·8699	1·0277	1·0972	1·1302	1·1463
0·7	θ		0·1389	0·2786	0·3503	0·3962	0·4273
	$F(\theta)$		0·8212	0·9702	1·0355	1·0665	1·0817
0·8	θ			0·2469	0·3316	0·3838	0·4188
	$F(\theta)$			0·9257	0·9868	1·0158	1·0300
0·9	θ			0·1667	0·2902	0·3575	0·4010
	$F(\theta)$			0·9012	0·9602	0·9883	1·0020
Max. Q	θ	0·0000	0·0000	0·0000	0·0000	0·0000	0·0000
	$F(\theta)$	0·4968	0·7891	0·8945	0·9473	0·9736	0·9868
In each case max. Q is respectively							
	Q	0·4073	0·7926	0·9361	0·9743	0·9884	0·9944

Appendix II

A detailed calculation with the same energy distribution used for Figure 4 is in Table 1. The energy distribution is Gaussian, with a standard deviation of 0·25 of the mean and energy limits at ± 2 standard deviations from the mean. Figure 4 applies at a radial distance of $R = 50\gamma_m$. Table 1 lists pairs of values of θ and $F(\theta)$. Because it is not possible to tabulate $F(\theta)$ directly against R and θ without many more values, subsidiary parameters P and Q are used, so the variation of $F(\theta)$ is evenly distributed throughout the range. We have defined

$$R = 2{\cdot}5 \times 2^P \gamma_m.$$

Q is a parameter specifying concentric paraboloids about the edge of the shadow region and is defined by

$$\tfrac{1}{4}R(1+\cos\theta)/\gamma_m = \frac{1}{1+a\sigma} + 1 + \tan[\tfrac{1}{4}\pi(3Q^2-1)],$$

where $a\sigma = 0{\cdot}5$ in this case.

The shadow is delineated by $Q = 0$ and the maximum Q is always less than 1·0. This maximum corresponds to $\theta = 0$. The values of $F(\theta)$ and Q, at $\theta = 0$, are listed at the bottom of each column.

Graphical interpolation in coordinates (P, Q) permits an evaluation of $F(\theta)$ to better than 1% over almost the entire field. For this purpose P and Q need to be calculated at the necessary points. The general form of the curves and rough magnitudes can be obtained by plotting against the associated values of R and θ. The program is available to anyone who needs more accurate results.